

Inductive Sustainment of a Field-Reversed Configuration Stabilized by Shaping, Magnetic Diffusion, and Finite-Larmor-Radius Effects

S. P. Gerhardt, E. V. Belova, M. Yamada, H. Ji, M. Inomoto,* Y. Ren,[†] and B. McGeehan
Princeton Plasma Physics Laboratory, Princeton University, P.O. Box 451 Princeton, New Jersey 08543, USA
 (Received 23 May 2007; published 14 December 2007)

Oblate field-reversed configuration (FRC) plasmas are sustained for up to 350 μs , or ≈ 15 poloidal flux-confinement times, in the magnetic reconnection experiment. The diamagnetic equilibrium is maintained in argon plasmas as a balance of an inward pinch and outward diffusion. Numerical and analytic models show that the observed stability is provided by a combination of plasma shaping, magnetic diffusion, and finite-Larmor radius effects. FRCs formed with lighter ions, which benefit less from these stabilizing effects, succumb to rapid instability and cannot be sustained.

DOI: [10.1103/PhysRevLett.99.245003](https://doi.org/10.1103/PhysRevLett.99.245003)

PACS numbers: 52.55.Lf, 52.35.Py

The field-reversed configuration (FRC) [1] is a toroidal plasma with unique physics properties: it is a diamagnetic equilibrium, supported by internal currents that are everywhere nearly perpendicular to the magnetic field. As a consequence, the ratio of plasma pressure to magnetic field pressure ($\beta \propto nT/B^2$) approaches unity. These properties have made the configuration attractive for a number of different technical applications (a fueling method for other magnetized plasmas [2], or as a fusion power-plant core [1] if significant stability and sustainment challenges can be overcome) and as a test-bed for high- β plasma science.

The sustainment of the FRC configuration has received increased theoretical and experimental attention over the past decade. For axially elongated (prolate) FRCs, rotating magnetic fields (RMF) [3] have been used to form and sustain the configuration. Computational [4] and experimental studies [5] have addressed sustainment by neutral-beam injection. The thermoelectric effect may provide a path to configuration sustainment, if the electron temperature gradient can be maintained [6]. For the oblate FRC with elongation $E < 1$ ($E = Z_S/R_S$, with R_S and Z_S the maximum radial and axial extents of the separatrix), inductive sustainment via a solenoid is attractive, since the FRC can be formed around the solenoid coil. Results from the TS-4 experiment have reported the ability to sustain an argon FRC with inductive current drive [7].

These efforts may be complicated by the fact that the FRC configuration possesses bad curvature everywhere (i.e., the field line curvature vector points opposite to the pressure gradient): the FRC should thus be unstable to a host of pressure-driven MHD instabilities [8] that could make sustainment difficult or impossible. The $n = 1$ versions of these modes (n is the toroidal mode number) are known as the tilt/shift modes, while the $n \geq 2$ versions are known as co-interchange modes [8,9]. While these modes have been observed and characterized in an oblate FRC [10], *prolate* FRCs are typically observed to be stable to these pressure-driven instabilities [1]. A likely cause of this stability is finite-Larmor-radius (FLR) stabilization [11]. The ions with their large orbits see a different average

electric field than the electrons, and thus have different electric drifts, introducing a stabilizing reactive effect.

In this Letter, we report long-time inductive sustainment and stability studies of oblate FRCs in the magnetic reconnection experiment (MRX) [12]. Argon FRCs have been sustained for up to 350 μs , corresponding to >15 flux-confinement times. There is a peaking of the plasma pressure during the solenoid current ramp due to an inward pinch, leading to a pressure profile consistent with the diamagnetic FRC equilibrium. Plasmas formed in nitrogen and neon display reduced stability, with helium and deuterium plasmas quickly becoming unstable. Stability analysis using simulation and analytic models shows that a combination of field shaping, resistive diffusion, and FLR effects provide stability in argon FRCs. These results demonstrate the longest yet sustainment of an oblate FRC, illuminate the sustainment process, and illustrate for the first time the stabilizing effects of resistivity and FLR-physics in an oblate FRC.

The MRX device is illustrated schematically in Fig. 1. Two spheromaks are formed at $Z \approx \pm 0.4$ m by pulsed currents in the flux-cores, and then allowed to merge at the ($Z = 0$) midplane, forming an oblate FRC. The current in a 68 turn solenoid is then ramped-up, inductively applying a toroidal electric field and sustaining the configuration. The solenoid is composed of two separate 34 turn coils, each inserted axially from the ends of the device; this design leaves a small gap (~ 2 cm) between the coils at the midplane, where some solenoid magnetic flux can “leak” out. Compensation coils are placed electrically in series with the solenoids to cancel the stray return flux of the solenoid. The combination of the midplane solenoid flux leakage and pushing force from the nearby shaping coils leads to a unique diamond shaped FRC. There are no nearby passive stabilizers.

These plasmas are studied using a comprehensive array of magnetic diagnostics. The large area array has coil triplets (B_R , B_Z , and B_ϕ measurements) on a 6×7 array at fixed toroidal angle. When combined with six poloidal flux loops on the solenoid surface, this array enables the

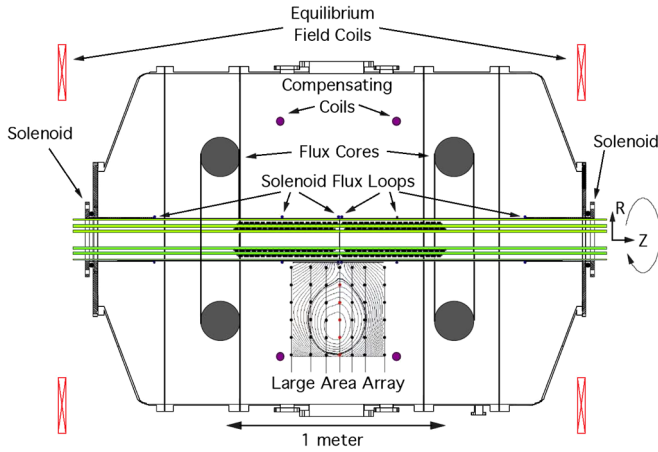


FIG. 1 (color online). Schematic of the MRX device, illustrating the major diagnostics and coils. The measured poloidal flux contours of a typical FRC are superimposed.

calculation of the plasma currents [J_R , J_Z , J_ϕ], poloidal magnetic flux (ψ), toroidal electric field ($E_\phi = (\partial\psi/\partial t)/2\pi R$), and plasma pressure (P , force balance). A second array, composed of 9 linear arrays with 5 coil triplets each, was inserted at the midplane ($Z = 0$) at 9 different toroidal angles. These “spoke probes” allow the study of midplane magnetic perturbations, indicative of plasma instabilities [10]. A triple Langmuir probe measured the midplane plasma density (n_e) and electron temperature. The ion temperature (T_i), inferred from limited Doppler spectroscopy along with pressure from force balance and the known electron pressure, was used to estimate the kinetic parameters defined later in this letter.

Sustained and unsustained argon FRCs are illustrated in Fig. 2, where the times here and throughout this letter are referenced to the end of the spheromak merging. Each column corresponds to a fixed time; the top row shows the two-dimensional profiles of toroidal field (colors) and poloidal flux (0.35 mWb between contours) for an inductively sustained case, while the bottom shows the same for an unsustained case. The two spheromaks are formed at $t \approx -140 \mu\text{s}$, propagate toward the midplane from their formation points on the left and right, merge, and form an

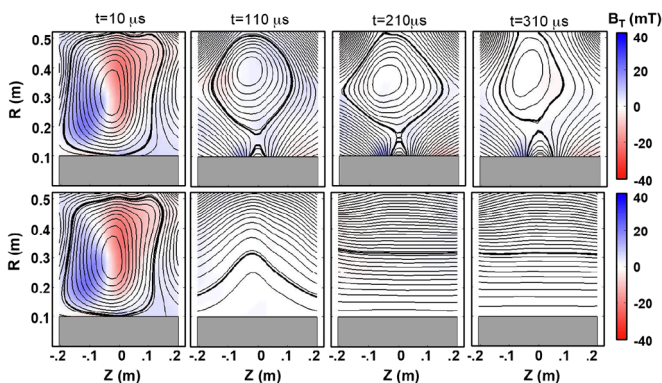


FIG. 2 (color online). The time evolution of sustained (top row) and unsustained (bottom row) argon FRCs.

FRC (at $t = 0 \mu\text{s}$). The FRC decays until the solenoid current ramp begins at $t \approx 40 \mu\text{s}$ (solenoid capacitor bank voltage $V_{OH} = 7.5 \text{ kV}$). The upper example then comes to a new sustained equilibrium for the $\approx 300 \mu\text{s}$ solenoid current ramp.

These argon (and krypton) FRCs can be sustained for the duration of the solenoid pulse, with no sign of performance limiting instabilities. This is illustrated by the scan over the solenoid firing voltage ($V_{OH} = 6, 7.5, \text{ and } 9 \text{ kV}$) at fixed argon fill pressure in Fig. 3. Figure 3(a) illustrates the poloidal flux trapped between the separatrix and the field null (ψ_t), while the solenoid magnetic flux is illustrated in Fig. 3(b), indicating the relative strength of the inductive drive. It is possible to sustain or increase the flux in the FRC, depending on the timing and voltage chosen for the solenoid pulse. In general, the duration of sustainment is limited only by the rise time of the solenoid waveform (the solenoid circuit was adjusted to provide the maximum possible pulse length); the maximum firing voltage was limited by imperfect compensation of the solenoid return flux. This good sustainment was not observed in lighter gasses, where, as discussed in detail below, instabilities severely limited the sustainment duration.

The method of sustaining this diamagnetic FRC equilibrium, which has no parallel currents, can be understood from the toroidal component of Ohm’s law: $E_\phi + (V \times B)_\phi = \eta_\perp J_\phi$, with V the plasma velocity, and η_\perp the

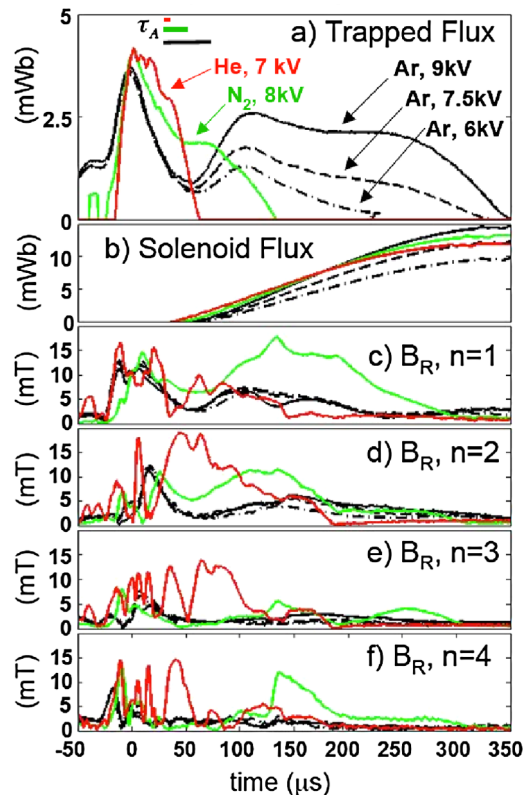


FIG. 3 (color online). Time evolution of the trapped poloidal flux, the solenoid flux, and $n = 1-4$ midplane perturbations to B_R , for different gasses.

plasma resistivity perpendicular to the magnetic field. Integrating this equation over the plasma surface yields the radial particle flux as [13]

$$\Gamma = n(\psi)\eta_{\perp}\left((2\pi)^2 \int R^2 \frac{ds}{B} \frac{\partial P}{\partial \psi} - n(\psi) \left[2\pi \int (RE_{\phi}) \frac{ds}{B} \right], \right. \quad (1)$$

where $n(\psi)$ is the plasma density, P the plasma pressure, and s the length along the magnetic field contour. The first term on the RHS represents outward classical diffusion, while the second term represents an inward pinch of particles. In steady state, the radial particle flux must be zero; the particle (and poloidal magnetic flux) balance of an inductively sustained FRC is determined by the balance between an inward pinch and outward diffusion.

This model of inductive sustainment has been verified by measuring the radial profiles of the plasma density and electron temperature with the Langmuir probe, for argon discharges with $V_{OH} = 7.5$ kV. The electron temperature profile is essentially flat at ~ 7 eV, a condition probably caused by the large radiated power in an argon plasma. Hence, the density and pressure profiles shapes are very similar. The data in Fig. 4(a)–4(d) illustrates the electron pressure profiles at 4 times, for cases with and without sustainment. The electron pressure is very high in the FRC state immediately after merging ($t = 35 \mu\text{s}$), but drops as the plasma decays. At $t = 85 \mu\text{s}$, the unsustained case has lost most of its pressure, while the sustained case is beginning to respond to the inductive loop voltage. The profiles quickly reacquire their peaked state, as predicted by the transport analysis based on Ohm's law, and maintain them for the duration of the sustainment.

The radial particle fluxes in (1) have been estimated, by mapping the measured density profile to poloidal flux, estimating the pressure gradient from force balance, estimating the resistivity from the ratio of the measured electric field and current density, and calculating the integrals in (1) from the measured electric and magnetic field distributions. During the steady state period, the inward and outward particle fluxes match to within 30%, with a value of $\sim 4 \times 10^{23} \text{ sec}^{-1}$. Volume integration of the density profile yields an estimated particle inventory of 1×10^{19}

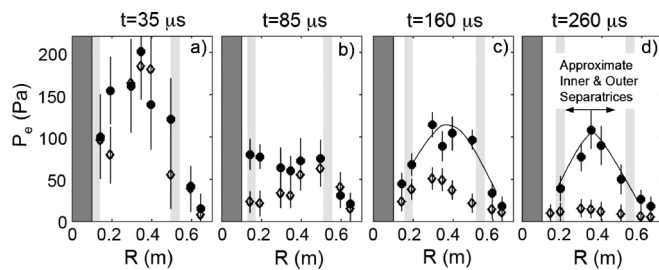


FIG. 4. (a)–(d) the time evolution of the electron pressure at the midplane, for sustained (closed symbols) and unsustained (open symbols) cases. See Fig. 2 for the corresponding equilibrium shapes.

electrons at $t = 160 \mu\text{s}$. These numbers yield a very rough estimate of the particle confinement time during sustainment phase as $\sim 25 \mu\text{s}$. This is similar to the more accurately measured poloidal flux-confinement time, defined as $\tau_{\psi} = \psi_t / (V_S - d\psi_t/dt)$, which is $\tau_{\psi} \approx 20 \mu\text{s}$ for this case ($V_S = \partial\psi_{\text{sep}}/\partial t$). The volume average resistivity, defined as $\eta_{\perp}^* = \int E_{\phi} dV / \int J_{\phi} dV$ is approximately $0.2 \text{ m}\Omega \cdot \text{m}$ for these plasmas; the resistivity profile is measured to be flat, as expected for a flat T_e profile. This measured value is very close to the Spitzer value of $\eta_{\perp} = 0.18 \text{ m}\Omega \cdot \text{m}$ based on an estimated $Z_{\text{eff}} = 1.5$. This $300 \mu\text{s}$ long discharge is thus sustained for $\approx 15\tau_{\psi}$.

The sustainment of argon FRCs is not limited by any instability. This is demonstrated in the bottom four frames of Fig. 3, where the midplane $n = 1$ –4 perturbations to B_R are illustrated as a function of time [the Alfvén times, $\tau_A = a/V_A$, with a the minor radius and $V_A = B/(\mu_0\rho)^{1/2}$ the Alfvén speed, are also indicated in frame (a)]. There is an initial burst of perturbations at $t = 0$, as the two spheromaks merge and settle into an FRC. The $n = 1$ and 2 modes begin to grow again as the solenoid ramp starts, then saturate and decrease in amplitude; the $n = 3$ and 4 modes show no substantial growth throughout this period. None of this activity noticeably impacts the evolution of the poloidal flux. The nitrogen FRCs (green traces) show very different properties, with only $\sim 50 \mu\text{s}$ of sustainment before the growth of magnetic perturbations causes the plasma to terminate. The instabilities are even more severe in helium (red traces), where virtually no period of sustainment is possible. Using the methodology described in Ref. [10], we have determined that these perturbations result from the axially polarized co-interchange mode. The N_2 and He discharges shown are typical in that many different toroidal mode numbers are simultaneously unstable; it is difficult to identify a single mode that leads to the discharge termination and the calculation of individual growth rates is difficult. However, the trend across many discharges is that strong $n = 1$ –4 mode activity in D_2 , He, N_2 , and Ne discharges leads to rapid discharge termination: discharges with large nonaxisymmetric perturbations are terminated more quickly than those without, and the time of maximum mode activity correlates strongly with time of discharge termination. The question is then to determine why the argon and krypton FRCs are stable.

We have identified three effects that play a role in stabilizing the argon and krypton FRCs. The first describes the stabilizing effect on the $n = 1$ tilt mode from the external field, as quantified by $n_{\text{decay}} = \frac{-R}{B_z} \frac{\partial B_z}{\partial R}$ [14]. If the plasma acquires a small tilt, it will feel a torque proportional to $(1 - n_{\text{decay}})$ in the direction of that tilt; for $n_{\text{decay}} > 1$, this torque will restore the plasma to its original position. The external field in these experiments had $n_{\text{decay}} \approx 0.7$ immediately after merging; the solenoid and compensating coils were configured such that $n_{\text{decay}} > 1$ once the solenoid flux exceeded ~ 3 mWb. The reduced

$n = 1$ amplitude during the solenoid ramp in argon discharges can thus be explained by the stabilizing effect of the external field. Furthermore, simulations [9] and experiment [10] indicate that shaping which eliminates the tilt also slows the growth rate of $n = 2$ modes. The $n = 1$ instabilities observed in lighter gasses are attributed to their rapid instability growth during early time with $n_{\text{decay}} < 1$.

A second stabilizing influence is due to resistivity; in a resistive plasma, the perturbed currents that drive the instability can be damped out more quickly than the instability can grow. For a global ideal mode, the governing parameter is the ratio of the resistive time to the Alfvén time (the Lundquist number, defined as $S = \mu_0 \alpha V_A / \eta$). The linear MHD stability of $n = 1-4$ modes was computed as a function of S using the HYM code [15], for a diamond shaped equilibria typical of these sustained FRCs. The $n = 1$ mode was found to be essentially stable for all S , as anticipated from the argument above. At large S (≈ 100), the $n = 2-4$ modes were all unstable, with the growth rate increasing with n from $\gamma_{n=2}/\gamma_A \approx 0.25$ to $\gamma_{n=4}/\gamma_A \approx 0.8$ ($\gamma_A = 1/\tau_A$). However, at Lundquist numbers typical of krypton plasmas ($S = 1-2$), the growth rates of all modes were $\gamma/\gamma_A < 0.1$; the observed good stability in krypton can thus likely be attributed to magnetic diffusion alone. For the $S = 4$ argon plasmas, the predicted growth rates for $n = 3$ and 4 modes were $\gamma/\gamma_A \approx 0.3$. The argon plasmas in Fig. 3, however, are sustained for $>6/\gamma_A$, or >2 growth times, in the presence of many potential seed perturbations, with no strong $n = 3$ and 4 growth.

This observation has motivated an examination of finite-Larmor-radius effects. The reactive effect noted in the introduction modifies the MHD dispersion relationship to read $\omega^2 - \omega^* \omega + \gamma_{\text{MHD}}^2 = 0$ [16], where γ_{MHD} is the MHD growth rate and $\omega_n^* = \mathbf{k} \cdot \mathbf{V}_D$, with $k = n/R_0$ and \mathbf{V}_D the diamagnetic drift velocity. Hence, an FLR stabilized mode should have $K_n = \gamma_{\text{MHD},n}/\omega_n^* < 1$. Using $\omega_n^* = \frac{nT_i}{R_0 \alpha B_{z,\text{sep}}}$ and $\gamma_{\text{MHD}} = \gamma_A/2$ as the typical growth rate for co-interchange modes in these FRCs (see above calculations and results in Ref. [10]), it can be seen that $K_n \propto \frac{B^2}{nT_i \sqrt{\rho}}$. Hence, a larger ion mass, higher toroidal mode number for the instability, and higher ion-temperatures decrease K_n and allow easier access to the FLR stabilized regime. Figure 5 shows the amplitudes of $n = 3$ and 4 perturbations plotted against K_3 and K_4 ; discharges with large values of K_3 and K_4 display large amplitudes of the associate instabilities, while K_3 & $K_4 < 1$ is typically sufficient to suppress these modes. Note that this scaling holds across many gasses, but also within the set of argon plasmas which display large $n = 4$ perturbations for $K_4 > 1$. In summary, the argon plasmas in MRX are stabilized by a combination of effects. Equilibrium shaping can largely eliminate the $n = 1$ tilt mode and assist with the $n = 2$ mode, and resistivity can slow the higher- n growth. FLR effects provide the final stabilizing contribution.

The poor stability observed in the MHD-regime deuterium and helium plasmas should not be a fundamental

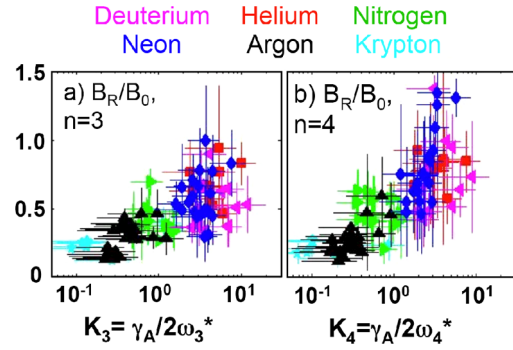


FIG. 5 (color online). The amplitude of $n = 3$ and 4 midplane B_R perturbations as a function of the relevant kinetic parameters.

impediment for oblate FRC development. Simulations and experiments have indicated that flexible shape control [10] and passive stabilizers can improve the MHD stability. When an energetic ion population is introduced into the simulations, complete stability is predicted; this idea is to be tested in the SPIRIT oblate FRC concept [17]. The present results, demonstrating the long-time inductive sustainment of an FRC, describing the sustainment process in detail, and illustrating the role of FLR effects and resistivity in providing stability to an oblate FRC, provide an important step along that development path.

This work is funded by the U. S. Department of Energy.

*Permanent address: Osaka University, Osaka, 565-0871, Japan.

†Permanent address: University of Wisconsin-Madison, Madison, WI 53706, USA.

- [1] M. Tuszewski, Nucl. Fusion **28**, 2033 (1988).
- [2] J.T. Slough and A.L. Hoffman, Phys. Plasmas **6**, 253 (1999).
- [3] A.L. Hoffman *et al.*, Phys. Plasmas **13**, 012507 (2006).
- [4] A.F. Lifschitz, R. Farengo, and A.L. Hoffman, Nucl. Fusion **44**, 1015 (2004).
- [5] T. Asai *et al.*, Phys. Plasmas **7**, 2294 (2000).
- [6] A. B. Hassam *et al.*, Phys. Rev. Lett. **83**, 2969 (1999).
- [7] E. Kawamori *et al.*, IAEA Fusion Energy Conference, Paper Ex P7-13, Chengdu, China, 2006.
- [8] A. Ishida *et al.*, Phys. Plasmas **1**, 4022 (1994).
- [9] E. V. Belova, S. C. Jardin, and H. Ji *et al.*, Phys. Plasmas **8**, 1267 (2001).
- [10] S.P. Gerhardt *et al.*, Phys. Plasmas **13**, 112508 (2006).
- [11] M.N. Rosenbluth, N.A. Krall, and N. Rostoker, Nucl. Fusion Suppl. **1**, 143 (1962).
- [12] M. Yamada *et al.*, Phys. Plasmas **4**, 1936 (1997).
- [13] S.P. Auerbach and W.C. Condit, Nucl. Fusion **21**, 927 (1981).
- [14] H. Ji *et al.*, Phys. Plasmas **5**, 3685 (1998).
- [15] E. V. Belova *et al.*, Phys. Plasmas **7**, 4996 (2000).
- [16] A. Ishida, H. Momota, and L. C. Steinhauer, Phys. Fluids **31**, 3024 (1988).
- [17] M. Yamada, H. Ji, and S.P. Gerhardt *et al.*, Plasma and Fusion Research **2**, 004 (2007).